Pair Interactions between Heterogeneous Spheres

Warwick J. C. Holt and Derek Y. C. Chan*

Department of Mathematics, University of Melbourne, Parkville, Victoria 3052, Australia

Received April 22, 1996. In Final Form: August 12, 1996[⊗]

Surface heterogeneities on colloidal particles may cause nonuniform charge distributions, which result in electrostatic potential profiles differing from those seen when charge is distributed uniformly. This, in turn, can give rise to attractive interactions between pairs of such surfaces which may be of greater magnitude and range than van der Waals attractions. We extend previous work on interactions between pairs of heterogeneous plates to pairs of spheres, with nonuniform constant potential or constant charge boundary conditions. As in the planar case, large attractive free energies can be obtained which are not present in the equivalent uniform surfaces. Additionally, large restraining torques can be found, affecting the rotational motion. These torques are not present in uniform charge models and may go some way toward explaining restraining torques found in some experimental systems.

1. Introduction

Pair interactions between colloidal particles are generally modeled by the work of Deryaguin, Landau, Verwey, and Overbeek, the DLVO theory, which considers the combined effect of electrostatic and van der Waals forces.[1−3] Experimental results for macroscopic surfaces have demonstrated the validity of this theory in many systems.[4] Other more recent studies, though, have shown the existence of forces other than those included in the DLVO theory.[5−7] Typically, these forces tend to be of shorter range than traditional electrostatic forces but of longer range than van der Waals forces. Some studies have proposed that these forces are caused by the hydrophobic nature of the surfaces,[6,8−11] and this goes some way toward explaining the phenomenon; but there are other systems for which this explanation does not seem feasible; for example, these forces have been observed in nonaqueous solvents and with nonhydrophobic adsorbed surfactants.[7,12]

One of the major simplifying assumptions of traditional DLVO theory is that the particle surfaces are assumed to be uniform. In practice, there are many cases in which such an assumption may not be valid. Surfaces previously regarded as uniform are shown to have a highly heterogeneous nature when examined closely by surface scanning techniques. For instance, cationic monolayers on mica are seen to be adsorbed in a "patchy" manner.[13]

There have been a number of papers[14−21] addressing the theory of nonuniform surfaces. The work in this paper builds on the work of Miklavic et al.,[19] which examined the interaction between two flat parallel plates, each divided into periodic rectangular cells with uniform rectangular "patches" within each cell. The boundary conditions specified on the patches and on the background differed. Cases were considered in which the patches were held at constant potential and the background held at a different constant potential which, when averaged over each cell, gave a net neutral system. Similar constant charge cases were also investigated, again for net neutral systems. It was found that attractions of much longer range than van der Waals forces occur between systems in which the surfaces were out of alignment.[19]

One would expect similar behavior if the two plates were replaced by a pair of spheres. In this paper we look at non-net neutral systems in both planar and spherical geometries, with periodic rectangular lattices on each surface. A periodic system such as this may also experience forces parallel (or, in the spherical system, tangent) to the surfaces, due to the energy differences between the system in different alignments. If the two surfaces are identical and aligned, for example, there will be a larger free energy than if the same surfaces are misaligned. A system in an energy minimum, therefore, will offer resistance to being shifted into an alignment of higher free energy.

Velegol et al.[22] have observed pairs of particles, while unattached, seeming to rotate as a rigid doublet, suggesting a great resistance to torques on individual particles. This is observed even when the particles are located in the secondary DLVO minimum. They propose that the restraining torque may be provided by having the system being in a local potential well due to heterogeneous charge distributions on the surface and that rotating the particles would force the system out of that state. In other words, the spheres are arranged so that they are (as close as possible, given the probable non-

* To whom correspondence should be addressed.

[⊗] Abstract published in *Advance ACS Abstracts,* November 1, 1996.

(1) Verwey, E. J. W.; Overbeek, J. Th. G., *Theory of the Stability of Lyophobic Colloids*; Elsevier: Amsterdam, 1948.
(2) Hunter, R. J. *Foundations of Colloidal Science, Volumes I and II*; Oxford University Press: Oxford, 1986.
(3) Russel, W. B.; Saville, D. A.; Schowalter, W. R. *Colloidal Dispersions*; Cambridge University Press: New York, 1989.
(4) Israelachvilli, J. N.; Adams, G. E. *J. Chem. Soc., Faraday Trans. 1* **1978**, *74*, *975*.
(5) Israelachvilli, J. N.; Pashley, R. M. *Nature* **1982**, *300*, 341.
(6) Pashley, R. M.; McGuiggan, P. M.; Ninham, B. W.; Parker, J. L. *Science* **1985**, *229*, 1088.
(7) Tsao, Y.-H.; Yang, S. X.; Evans, D. F.; Wennerström, H. *Langmuir* **1991**, *7*, 3154.
(8) Podgornik, F. *J. Chem. Phys.* **1989**, *91*, 5840.
(9) Attard, P. J., *J. Chem. Phys.* **1989**, *93*, 6441.
(10) Christenson, H. K.; Claesson, P. M. *Science* **1988**, *239*, 390.
(11) Ducker, W. A.; Xu, Z.; Clarke, D. R.; Israelachvilli, J. N. *J. Am. Ceram. Soc.* **1994**, *77*, 437.
(12) Tsao, Y.-H.; Evans, D. F.; Wennerström, H. *Science* **1993**, *262*, 547.
(13) Nishimura, S.; Scales, P. J.; Biggs, S. R.; Healy, T. W. *Colloids Surf. A: Physiochem. Eng. Aspects* **1995**, *103*, 289.
(14) Richmond, P. *J. Chem. Soc., Faraday Trans. 2* **1974**, *70*, 1066.
(15) Richmond, P. *J. Chem. Soc., Faraday Trans. 2* **1975**, *71*, 1154.
(16) Nelson, A. P.; McQuarrie, D. A. *J. Theor. Biol.* **1975**, *55*, 13.
(17) Kuin, A. J. *Faraday Discuss. Chem. Soc.* **1990**, *90*, 235.
(18) Vreeker, R.; Kuin, A. J.; Den Boer, D. C.; Hoekstra, L. L.; Agterof, W. G. M. *J. Colloid Interface Sci.* **1992**, *154*, 138.
(19) Miklavic, S. J.; Chan, D. Y. C.; White, L. R.; Healy, T. W. *J. Phys. Chem.* **1994**, *98*, 9022.
(20) Miklavcic, S. J. *J. Chem. Phys.* **1995**, *103*, 4794.
(21) Grant, M. L.; Saville, D. A. *J. Colloid Interface Sci.* **1995**, *171*, 35.
(22) Velegol, D.; Anderson, J. L.; Garoff, S. *Langmuir* **1996**, *12*, 4103.

S0743-7463(96)00389-7 CCC: $14.00

periodicity of the surfaces) out of alignment. They also point out that even relatively shallow wells could result in large rigidity torques.

This paper investigates the potential, pressure and free energy between pairs of plates made up of patched cells with different values for the charge or potential on the patches and the background. Furthermore, we use the Deryaguin approximation to extend this work to pairs of spheres, allowing us to investigate restraining torques of couplets such as those studied by Velegol et al.[22]

2. Electrostatic Interaction for Heterogeneous Plates

There are four possible choices of electrostatic boundary conditions for this problem. We can consider cases in which the background surface is held at either constant potential or constant charge while the surfaces are brought together. The surfaces of the patches can be held at either constant potential or constant charge. The easier cases are the ones in which the background and patch areas have the same type of boundary condition: either both are constant potential or both are constant charge. These are the cases we shall consider here; the mixed boundary value cases shall be left for a future paper.

We follow the technique used by Miklavic et al.[19] for planar surfaces held at either constant potential or constant charge. We allow the values of the surface potential or surface charge to take on two possible values: one for the boundary condition on the patch, and one for the boundary condition on the remainder of the surface. In essence, this is equivalent to superimposing a periodic distribution of sources over a uniform surface. Due to this periodicity, the sources can be represented as Fourier series.

The electrostatic interaction is considered under the linearized Poisson−Boltzmann (or Debye−Hückel) model. A perturbation treatment of nonlinear effects has recently been proposed.[20] Using the linear thermodynamic charging integration, Miklavic et al.[19] obtained expressions for the free energy per unit area on each surface. The interaction free energy per unit area for two constant potential surfaces is then given by

$$V_p(h) = \frac{\epsilon_2}{8\pi}\left\{\sum_{\mathbf{k}_L}\frac{-q_L\psi^L_{\mathbf{k}}}{\sinh(q_L h)}[(\psi^L_{-\mathbf{k}}e^{-q_L h}) - \sum_{\mathbf{k}_R}\psi^R_{\mathbf{k}}C_R(\mathbf{k}_L, \mathbf{k}_R)] + \sum_{\mathbf{k}_R}\frac{-q_R\psi^R_{\mathbf{k}}}{\sinh(q_R h)}[\psi^R_{-\mathbf{k}}e^{-q_R h} - \sum_{\mathbf{k}_L}\psi^L_{\mathbf{k}}C_L(\mathbf{k}_L, \mathbf{k}_R)]\right\} \quad (1)$$

Here, ϵ_2 is the dielectric constant of the medium of thickness h that separates the two plates; $\psi^L_{\mathbf{k}}$ are the (known) Fourier coefficients for the specified surface potential distributions, $\psi(x,y)$ on the left surface; $\mathbf{k}_L$ is a reciprocal lattice vector (or wave number) that depends on the precise form of the two-dimensional distribution of the specified surface potential on the planes. q_L is a modified inverse screening length, given by

$$q_L = \sqrt{\kappa^2 + \mathbf{k}_L^2} \quad (2)$$

where κ is the usual inverse Debye length of an electrolyte with number density n_i and valence z_i of species i, given by

$$\kappa = \sqrt{\frac{4\pi e^2\sum n_i z_i}{\epsilon_2 k_B T}} \quad (3)$$

Here e is the protonic charge, k_B is the Boltzmann constant, and T is the absolute temperature. Analogous definitions exist for the variables with the subscript $L \rightarrow R$ corresponding to the right-hand surface.

Finally, we have the definition

$$C_L(\mathbf{k}_L, \mathbf{k}_R) = \frac{1}{A_L}\int_{A_L} e^{i(\mathbf{k}_L + \mathbf{k}_R)\cdot\mathbf{s}}\, d\mathbf{s} \quad (4)$$

and an analogous definition for $C_R(\mathbf{k}_L,\mathbf{k}_R)$; note that these quantities reduce to Kronecker delta functions in the case of identical lattices.

Similarly, Miklavic et al.[19] treated the case of constant charge surfaces. The corresponding expression for the interaction free energy per unit area is

$$V_c(h) = 2\pi \times \left\{\sum_{\mathbf{k}_L}\frac{\sigma^L_{\mathbf{k}}e^{-q_L h}\,[\sigma^L_{-\mathbf{k}}\Delta^L_{23}(1+\Delta^L_{21})e^{-q_L h} + (1+\Delta^L_{23})\sum_{\mathbf{k}_R}\sigma^R_{\mathbf{k}}C_R(\mathbf{k}_L, \mathbf{k}_R)]}{N_L(\epsilon_2 q_L + \epsilon_1 k_L)} + \sum_{\mathbf{k}_R}\frac{\sigma^R_{\mathbf{k}}e^{-q_R h}\,[\sigma^R_{-\mathbf{k}}\Delta^R_{21}(1+\Delta^R_{23})e^{-q_R h} + (1+\Delta^R_{21})\sum_{\mathbf{k}_L}\sigma^L_{\mathbf{k}}C_L(\mathbf{k}_L, \mathbf{k}_R)]}{N_R(\epsilon_2 q_R + \epsilon_3 k_R)}\right\} \quad (5)$$

where

$$N_j = 1 - \Delta^j_{21}\Delta^j_{23}e^{-2q_j h} \qquad j = L, R \quad (6)$$

and

$$\Delta^j_{2i} = \frac{\epsilon_2 q_j - \epsilon_i k_j}{\epsilon_2 q_j + \epsilon_i k_j} \qquad j = L, R; \qquad i = 1, 3 \quad (7)$$

Again, the $\sigma_{\mathbf{k}}$ represent Fourier coefficients for the specified surface charge distributions. ϵ_1 and ϵ_3 are the dielectric constants for the left and right hand half-spaces, respectively. Note also that $k_j = |\mathbf{k}_j|$.

If we assume that the two interacting surfaces are identical, so that the lattices are identical (C_L and C_R become Kronecker delta functions and $\epsilon_1 = \epsilon_3$), these expressions simplify considerably. For constant potential surfaces we have

$$V_p(h, \mathbf{d}) = \frac{\epsilon_2}{4\pi}\sum_{\mathbf{k}}\frac{q\psi_{-\mathbf{k}}\psi_{\mathbf{k}}}{\sinh(qh)}[\cos(\mathbf{k}\cdot\mathbf{d}) - e^{-qh}] \quad (8)$$

while for two plates held at constant charge we get

$$V_c(h, \mathbf{d}) = 8\pi\epsilon_2\sum_{\mathbf{k}}\frac{qe^{-qh}\,\sigma_{-\mathbf{k}}\sigma_{\mathbf{k}}}{N}\left[\frac{\cos(\mathbf{k}\cdot\mathbf{d}) + \Delta e^{-qh}}{(\epsilon_2 q + \epsilon_1 k)^2}\right] \quad (9)$$

In these two eqs we have dropped all unneccessary subscripts and superscripts, so that $\mathbf{k}_L = \mathbf{k}_R = \mathbf{k}$, $q_L = q_R = q$, $N_L = N_R = N$, and $\Delta^{L,R}_{21} = \Delta^{L,R}_{23} = \Delta$.

Note the presence of a phase factor, $\cos(\mathbf{k}\cdot\mathbf{d})$, which arises from the lateral displacement, $\mathbf{d} = (d_x,d_y)$ of the two lattices. Naturally, this results in periodic variations or peaks and troughs in the free energy, as we slide the plates over each other at constant separation.

The disjoining pressure between the two plates is given by the negative derivative of the interaction free energy with respect to separation h, and the result for constant

potential is

$$P_{z,p}(h, \mathbf{d}) = \frac{\epsilon_2}{4\pi}\sum_{\mathbf{k}} \frac{q^2\psi_{-\mathbf{k}}\psi_{\mathbf{k}}\,[\cos(\mathbf{k}\cdot\mathbf{d})\cosh(qh) - 1]}{\sinh^2(qh)} \tag{10}$$

and for constant charge is

$$P_{zc}(h, \mathbf{d}) = 8\pi \sum_{\mathbf{k}} \left(\frac{\epsilon_2 q}{N}\right)^2 e^{-qh}\sigma_{-\mathbf{k}}\sigma_{\mathbf{k}} \left[\frac{(1 + \Delta^2 e^{-2qh})\cos(\mathbf{k}\cdot\mathbf{d}) + \Delta e^{-qh}}{(\epsilon_2 q + \epsilon_1 k)^2}\right] \tag{11}$$

We consider the simplest two-dimensional model, in which rectangular patches of dimensions $2b_x \times 2b_y$ are placed in the center of periodic rectangular cells of dimensions $2a_x \times 2a_y$, covering each surface. A reciprocal lattice vector $\mathbf{k}$ for this geometry is

$$\mathbf{k} = (k_x, k_y) = \left(\frac{\pi i}{a_x}, \frac{\pi j}{a_y}\right) \tag{12}$$

and summation over such vectors becomes a summation over integer values of i and j, with $i, j = 0, 1, 2, \ldots$. Also

$$\mathbf{k}\cdot\mathbf{d} = \pi\left\{\frac{id_x}{a_x} + \frac{jd_y}{a_y}\right\} \tag{13}$$

For the chosen rectangular geometry, the Fourier coefficients in eq 1 can now be determined. If we let $\gamma_{\mathbf{k}}$ represent either $\psi_{\mathbf{k}}$ for constant potential surfaces or $\sigma_{\mathbf{k}}$ for constant charge surfaces, then the Fourier decomposition for square patches on square cells is given by

$$\gamma_{\mathbf{k}} = \gamma_p \frac{\sin\left(\frac{\pi i b_x}{a_x}\right)}{\pi i} \frac{\sin\left(\frac{\pi j b_y}{a_y}\right)}{\pi j} + \delta_{\mathbf{k},\mathbf{0}}\gamma_b \tag{14}$$

We use the limit $\lim_{x\to 0}((\sin x)/x) = 1$ to evaluate the components when either i or j are equal to zero. γ_b and γ_p represent the values of the background and patch boundary conditions, respectively. $\delta_{\mathbf{k},\mathbf{0}}$ is the Kronecker delta function; the value of the background boundary condition only contributes to the first of the Fourier components, the $\mathbf{k} = \mathbf{0}$ term. The $\mathbf{k} = \mathbf{0}$ terms for the interaction free energy and disjoining pressure correspond to the familiar result for a uniformly charged surface having the area averaged net charge or potential of the heterogeneous patchy surface considered here. So the effect of the surface heterogeneities can be isolated by retaining only the $\mathbf{k} \neq \mathbf{0}$ terms.

In addition, we can determine the shear stress between the two plates or the force per unit area parallel to the plate surfaces. The shear stress will be zero both when the two surface lattices are exactly out of register with each other and when the two surfaces are exactly in register. The former case, i.e., $\mathbf{d} = \mathbf{a} = (a_x, a_y)$, corresponds to a local energy minimum; the latter, when $\mathbf{d} = \mathbf{0}$, is when the system is in a local energy maximum. For other values of the displacement vector $\mathbf{d}$, there will be a transverse force driving the surface toward the nearest local minimum.

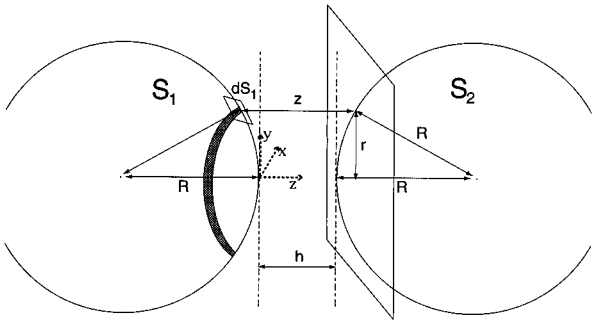

Figure 1. Geometry of the Deryaguin approximation for spheres, where interactions are approximated by an integral of plate−plate interactions at separation z.

The shear stress can be found by taking the negative gradient of the interaction free energy in the x and y directions. This gives for the constant potential case

$$\mathbf{P}_{trp}(h, \mathbf{d}) = \frac{\epsilon_2}{4\pi}\sum_{\mathbf{k}} \frac{q\psi_{-\mathbf{k}}\psi_{\mathbf{k}}}{\sinh(qh)} \sin(\mathbf{k}\cdot\mathbf{d})\mathbf{k} \tag{15}$$

and for the constant charge case

$$\mathbf{P}_{trc}(h, \mathbf{d}) = 4\pi\epsilon_2 \sum_{\mathbf{k}} \frac{qe^{-qh}}{N} \frac{\sigma_{-\mathbf{k}}\sigma_{\mathbf{k}} \sin(\mathbf{k}\cdot\mathbf{d})}{(\epsilon_2 q + \epsilon_1 k)^2}\mathbf{k} \tag{16}$$

Note that these stresses are vectors in the $x - y$ plane and are made up of sums of components with directions determined by the wave vectors $\mathbf{k}$. This also means that the shear stresses have an inverse relationship to the cell sizes $\mathbf{a}$.

From eq 13 we can also see that if the two components of $\mathbf{d}$ are integer multiples of their respective $\mathbf{a}$ components, then the shear stress will be zero, since $\sin(\mathbf{k}\cdot\mathbf{d}) = 0$. This corresponds to the plates being exactly in or exactly out of register, or in register in one dimension and out of register in the other.

3. Interactions between Heterogeneous Spheres

We now use the Deryaguin method to deduce the interaction between two spheres of radius R with heterogeneous surface charges or potentials. This method is valid in the limit $\kappa R \gg 1$ and $h/R \ll 1$, where h is the distance of closest approach between the spheres.

We use the geometry of Figure 1 and consider the interaction between an area element dS_1 on the surface of sphere 1 and a planar half-space located a distance z away, which approximates sphere 2. If we take the free energy per unit area between two planes to be $V(z)$, then

$$dV^{sp} \approx V(z)\, dS_1 \tag{17}$$

is the interaction energy between element dS_1 and sphere 2. This expression becomes increasingly accurate as the radii of the spheres approach infinity. We can obtain the total interaction free energy between the spheres by integrating over the surface of sphere 1

$$V^{sp}(h) = \int_{S_1} V(z)\, dS_1 \tag{18}$$

From Figure 1, it can clearly be seen that

$$2R + h = z + 2\sqrt{R^2 - r^2} \tag{19}$$

and within the limit of the Deryaguin method we have

$$dz = \frac{2r\,dr}{\sqrt{R^2 - r^2}} \approx \frac{2r}{R}\,dr \tag{20}$$

and

$$dS_1 \approx 2\pi r\,dr \tag{21}$$

This gives the final result

$$V^{sp}(h) = \pi R \int_h^\infty V(z)\,dz \tag{22}$$

If we apply this to the general interaction free energy between two constant potential plates, via eq 1, we can obtain an expression for the general interaction free energy between two spheres held at constant potential

$$V_p^{sp}(h) = \frac{-\epsilon_2 R}{8}\left\{\sum_{\mathbf{k}_L}\psi_{\mathbf{k}}^L\left[\psi_{-\mathbf{k}}^L \ln\left|1 - e^{-2q_L h}\right| + \ln\left|\tanh\frac{q_L h}{2}\right|\sum_{\mathbf{k}_R}\psi_{\mathbf{k}}^R C_R(\mathbf{k}_L, \mathbf{k}_R)\right] + \sum_{\mathbf{k}_R}\psi_{\mathbf{k}}^R\left[\psi_{-\mathbf{k}}^R \ln\left|1 - e^{-2q_R h}\right| + \ln\left|\tanh\frac{q_R h}{2}\right|\sum_{\mathbf{k}_L}\psi_{\mathbf{k}}^L C_L(\mathbf{k}_L, \mathbf{k}_R)\right]\right\} \tag{23}$$

As before, C_L and C_R are defined by eq 4. If we assume the lattices are identical, this again simplifies.

$$V_p^{sp}(h, \mathbf{d}) = \frac{-\epsilon_2 R}{4}\sum_{\mathbf{k}}\psi_{-\mathbf{k}}\psi_{\mathbf{k}}\left\{\ln\left|\tanh\frac{qh}{2}\right|\cos(\mathbf{k}\cdot\mathbf{d}) + \ln(1 - e^{-2qh})\right\} \tag{24}$$

Similarly, we can use eq 5 to obtain the general interaction free energy between two spheres at constant charge

$$V_c^{sp}(h) = -2\pi^2\epsilon_2 R\left\{\sum_{\mathbf{k}_L}\frac{\sigma_{\mathbf{k}}^L}{(\epsilon_2 q_L + \epsilon_1 k_L)}\left[\frac{\sigma_{-\mathbf{k}}^L \ln(N_L)}{(\epsilon_2 q_L - \epsilon_1 k_L)} + \sum_{\mathbf{k}_R}\frac{\sigma_{\mathbf{k}}^R C_R(\mathbf{k}_L, \mathbf{k}_R)\eta_L}{(\epsilon_2 q_L + \epsilon_3 k_L)}\right] + \sum_{\mathbf{k}_R}\frac{\sigma_{\mathbf{k}}^R}{(\epsilon_2 q_R + \epsilon_3 k_R)}\left[\frac{\sigma_{-\mathbf{k}}^R \ln(N_R)}{(\epsilon_2 q_R - \epsilon_3 k_R)} + \sum_{\mathbf{k}_L}\frac{\sigma_{\mathbf{k}}^L C_L(\mathbf{k}_L, \mathbf{k}_R)\eta_R}{(\epsilon_2 q_R + \epsilon_1 k_R)}\right]\right\} \tag{25}$$

where for $j = L$ or R

$$\eta_j = \begin{cases} \dfrac{1}{\sqrt{\Delta_{21}^j\Delta_{23}^j}} \ln\left|\dfrac{1 - \sqrt{\Delta_{21}^j\Delta_{23}^j}e^{-q_j h}}{1 + \sqrt{\Delta_{21}^j\Delta_{23j}}\,e^{-q_j h}}\right| & \text{for } \Delta_{21}^j\Delta_{23j} > 0 \\ -2e^{-q_j h} & \text{for } \Delta_{21}^j\Delta_{23}^j = 0 \\ \dfrac{2}{\sqrt{|\Delta_{21}^j\Delta_{23}^j|}} \arctan\left(\sqrt{|\Delta_{21}^j\Delta_{23}^j|}e^{-q_j h}\right) & \text{for } \Delta_{21}^j\Delta_{23}^j < 0 \end{cases} \tag{26}$$

and for identical lattices on identical spheres (i.e. having the same dielectric constant, $\epsilon_1 = \epsilon_3$) the energy becomes

$$V_c^{sp}(h, \mathbf{d}) = 4\pi^2\epsilon_2 R\sum_{\mathbf{k}}\frac{\sigma_{-\mathbf{k}}\sigma_{\mathbf{k}}}{(\epsilon_1 k)^2 - (\epsilon_2 q)^2} \times \left[\ln\left(\frac{1 - \Delta e^{-qh}}{1 + \Delta e^{-qh}}\right)\cos(\mathbf{k}\cdot\mathbf{d}) + \ln(N)\right] \tag{27}$$

where we have dropped all unneccessary subscripts and superscripts in the same manner as in the two plate calculation. Again, the results depend on the phase factor ($\mathbf{k}\cdot\mathbf{d}$), and the interaction free energy will depend upon the alignment of the two surfaces. As in the two-plate system, there will be a transverse force and resultant torques on the particles in addition to the normal force acting along the line of centers. This additional force will act to drive the orientation of the spheres toward a local free energy minimum at constant separation.

Once again we consider rectangular patches on rectangular cells, so that the sum over $\mathbf{k}$ is actually a double sum over integer values of i and j, with $\mathbf{k}$ being defined by eq 12.

From eqs 24 and 27 for the free energy, we can determine the transverse forces, and hence the rotational torques. The transverse force is found by taking the negative gradient of the energy with respect to the two transverse directions, x and y (which define the plane in which the relative displacement vector lies). We are interested in the force at the point of closest approach of the spheres, i.e., at separation h. The transverse forces can also be obtained by applying the Deryaguin technique to eqs 15 and 16, as the transverse force in a two sphere interaction can be found from the shear stress in the corresponding two plate case. The results are identical.

This results in the following expressions for the transverse force vector for the constant potential case

$$\mathbf{F}_{trp}^{sp}(h, \mathbf{d}) = -\frac{\epsilon_2 R}{4}\sum_{\mathbf{k}}\psi_{-\mathbf{k}}\psi_{\mathbf{k}} \ln\left|\tanh\frac{qh}{2}\right| \sin(\mathbf{k}\cdot\mathbf{d})\mathbf{k} \tag{28}$$

and the constant charge case

$$\mathbf{F}_{trc}^{sp}(h, \mathbf{d}) = -4\pi^2 R\epsilon_2\sum_{\mathbf{k}}\ln\left(\frac{1 - \Delta e^{-qh}}{1 + \Delta e^{-qh}}\right)\frac{\sigma_{-\mathbf{k}}\sigma_{\mathbf{k}} \sin(\mathbf{k}\cdot\mathbf{d})}{(\epsilon_1 k)^2 - (\epsilon_2 q)^2}k \tag{29}$$

The torque can be obtained from the transverse force vector by the usual expression $\mathbf{T} = R\hat{\mathbf{z}} \times \mathbf{F}$, where the vector $R\hat{\mathbf{z}}$ is the radius vector from the center of sphere 1 toward the center of sphere 2. This vector defines the z direction, and the torque will therefore lie at right angles to the transverse force at $x = y = 0$ (the point of closest approach of the spheres, where their surfaces are locally parallel). The expression for the torque for two identical constant potential spheres is

$$\mathbf{T}_p^{sp}(h, \mathbf{d}) = \frac{-\epsilon_2 R^2}{4}\sum_{\mathbf{k}}\psi_{-\mathbf{k}}\psi_{\mathbf{k}} \ln\left|\tanh\frac{qh}{2}\right| \sin(\mathbf{k}\cdot\mathbf{d})(k_y\hat{\mathbf{x}} - k_x\hat{\mathbf{y}}) \tag{30}$$

and for the equivalent constant charge spheres

$$\mathbf{T}_c^{sp}(h, \mathbf{d}) = -4(\pi R)^2\epsilon_2\sum_{\mathbf{k}}\ln\left(\frac{1 - \Delta e^{-qh}}{1 + \Delta e^{-qh}}\right)\frac{\sigma_{-\mathbf{k}}\sigma_{\mathbf{k}} \sin(\mathbf{k}\cdot\mathbf{d})}{(\epsilon^1 k)^2 - (\epsilon_2 q)^2}(k_y\hat{\mathbf{x}} - k_x\hat{\mathbf{y}}) \tag{31}$$

From these results we make two observations. The first is that the magnitudes of the torques are amplified by a factor R/a when compared to the interaction free energies, since the wave vector components, k_x and k_y are proportional to $1/a$. Since by construction the radii of the spheres are assumed to be far greater than the cell size a, large torque values are obtainable with relatively small values for the free energies. Additionally, we note that the $\mathbf{k} = \mathbf{0}$ terms in eqs 30 and 31 equal zero because the $\mathbf{k} = \mathbf{0}$ terms correspond to contributions from the homogeneous surface charge or potential, and we do not expect a contribution to the torque from such terms. This means that the leading order terms in the torque calculation are the $(i, j) = (1, 0)$ or $(0, 1)$ terms. The appearance of $\sin(\mathbf{k}\cdot\mathbf{d})$ rather than $\cos(\mathbf{k}\cdot\mathbf{d})$ means that the maxima and minima will not be found when the surfaces are exactly in and out of alignment, as with the free energy and pressure. On the contrary, at these orientations, the torque will be zero; the largest torque magnitudes will occur at some place between these extremes, depending upon the values of **a** and **b**. Physically, the value of the torque at these points represents the maximum amount of torque required to twist the spheres freely; this is the maximum "restraining torque". Note that less torque is required to twist the spheres from an out-of-alignment state along one of its axes than along a diagonal. This is a result of the nature of the rectangular surface lattice chosen in our model.

4. Results and Analysis

We present results for a variety of different boundary conditions. The bulk of the results shall be given for square patches on regular square lattice cells, but we also investigate the effect of modifying the patch shape while retaining the same overall area.

As discussed earlier, the $\mathbf{k} = \mathbf{0}$ term in the interaction energy or force is due to the area averaged surface charge or potential distribution. This contribution, together with van der Waals interactions, forms the basis of the familiar classical DLVO theory of colloidal interactions. In the present model, effects of surface heterogeneities are all contained in the $\mathbf{k} \neq \mathbf{0}$ terms, and we shall concentrate our discussion on this latter contribution.

The two plate problem, as analyzed in section 2, has previously had a significant numerical treatment.[19] We therefore present results concentrating upon the two identical sphere setup derived in section 3. We also note that substantial simulation of both planar and spherical systems has produced results with similar essential characteristics in corresponding systems. Most of the comments made below concerning the two sphere systems (excepting, naturally, those specifically referring to the spherical geometry) apply equally to the corresponding two plate cases.

Initially we will look at the dependence of the free energy on separation, and we keep $\mathbf{d} = \mathbf{a}$, so that the attraction between the two surfaces is at a maximum. In Figure 2 we show the effects of altering the patch size (**b**) and the cell size (**a**) while keeping other parameters fixed. For comparison, we choose the nonretarded Hamaker formula for the van der Waals interaction: $-A/(12h)$, with a Hamaker constant $A = 10^{-20}$ J. This value of the Hamaker constant will be used in all results given herein.

Figure 2a shows the $\mathbf{k} \neq \mathbf{0}$ terms for three systems with square patches on square cells, held at constant potentials. Here **b** is held fixed, with $b_x = b_y = 50$ Å square, and the cell size is a square with $a_x = a_y$ given in the legend (60, 100, and 200 Å). The net surface potential is the same for all cases (25 mV) and this means that the value of the patch potential at infinite separation will be greater for a larger cell size, since the patch area/background area ratio will be lower. In Figure 2b we show the same results for constant charge systems which have the same properties at infinite separation as for the constant potential case. In other words, at infinite separation the system is identical to the system in Figure 2a with potentials distributed on square patches to give a net potential of 25 mV, except that the charge density on each surface is then held fixed as the surfaces are brought together. The results clearly show that the decay length varies with cell size: the larger the cell size, the greater the heterogeneous contribution to the free energy, and the longer the decay length. This is in line with the definition of q in eq 2 as a modified decay length. As $\mathbf{a} \rightarrow \mathbf{b}$, the surface will appear more homogeneous, and the $\mathbf{k} \neq \mathbf{0}$ terms should vanish. The constant potential and charge curves converge as the separation increases, but at close approach the constant potential curves dip sharply where the constant charge curves flatten off (in fact, for large cell size and small separation, the heterogeneous free energy begins to increase). The dot−dash line shows the van der Waals interaction. Clearly for sufficiently large cell sizes the hetergeneous electrostatic component displays both greater magnitude and greater range than the van der Waals interaction.

In these and most other cases, the modified decay length, q^{-1}, varies linearly with cell size. This arises directly from eq 2. This will hold so long as the κ term in the equation remains relatively small. When $\kappa^{-1} \approx a/2$ or smaller, the modified decay length will also depend on the value of κ.

In parts c and d of Figure 2 we show the heterogeneous free energy curves for three systems in which the cell size, **a**, is kept fixed, $a_x = a_y = 100$ Å, but the patch size **b** is modified. Figure 2c is for constant potential; Figure 2d is for constant charge. Note that for large separation h, the curves all have the same decay length. This confirms that the effective decay length depends on cell size as well as salt concentration. Again, the magnitude of the heterogeneous energy is greatest when the patch size is smallest and least as the surfaces approach homogeneity. Also note again that when we have small patch sizes relative to the size of the cell (Figure 2d), the heterogeneous free energy becomes repulsive.

In parts e and f of Figure 2 we show (for constant potential and constant charge, respectively) the effects of modifying the shape of the patch. In all three curves $a_x = a_y = 100$ Å, and the overall area of the patch, $4b_x b_y$ remains fixed at 10 000 Å^2. The solid line is the result pertinent to a square patch; the short dashed line represents the results for a surface comprised of striped heterogeneities, with the long dashed line showing the results for an intermediate case. As can be seen in both figures, the change in the free energy curve is minimal; interestingly, though, the magnitude of the heterogeneous energy is lowest for the square patch and increases as one deviates further from a square shape. In this sense studying square patches on square cells (in the case $\mathbf{d} = \mathbf{a}$) should give us a lower bound on the heterogeneous contribution, at least for rectangular symmetries.

Similar trends to those seen in Figure 2 are also seen in the variation of pressure against separation for different cell and patch sizes; namely that the slope of the log(pressure) vs separation curve is a sensitive function of the cell size but is insensitive to the patch shape.

In Figure 3 we show contributions to the interaction free energy between spheres from (i) the $\mathbf{k} = \mathbf{0}$ homogeneous electrostatic term, (ii) the van der Waals interaction, and (iii) the electrostatic interaction for charge or potential heterogeneities (the $\mathbf{k} \neq \mathbf{0}$ term). The last contribution will depend on the relative lateral displacement of the

Fig. 2a)

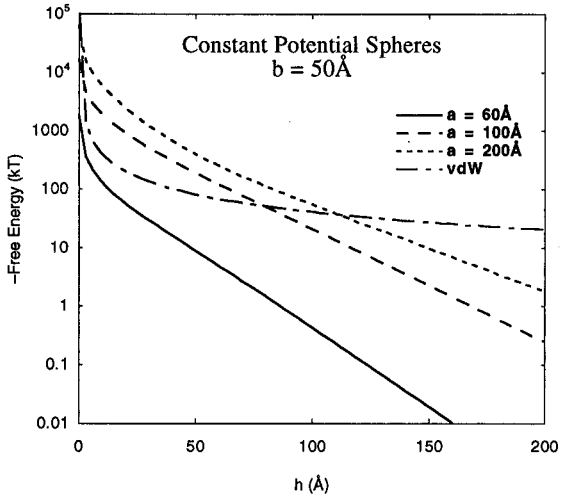

Fig. 2b)

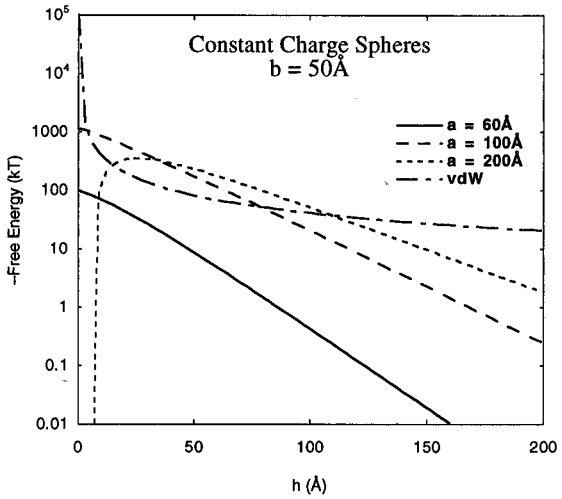

Fig. 2c)

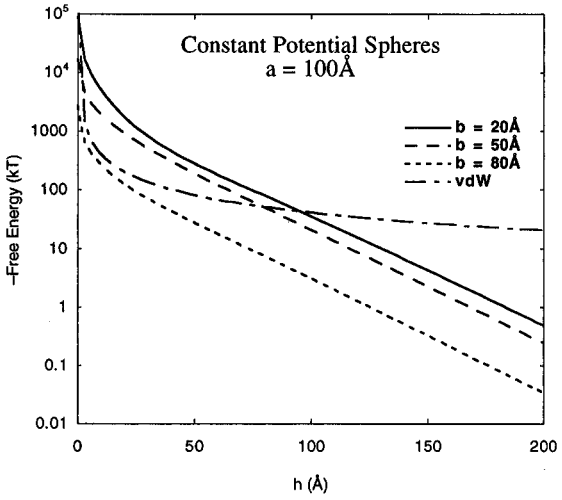

Fig. 2d)

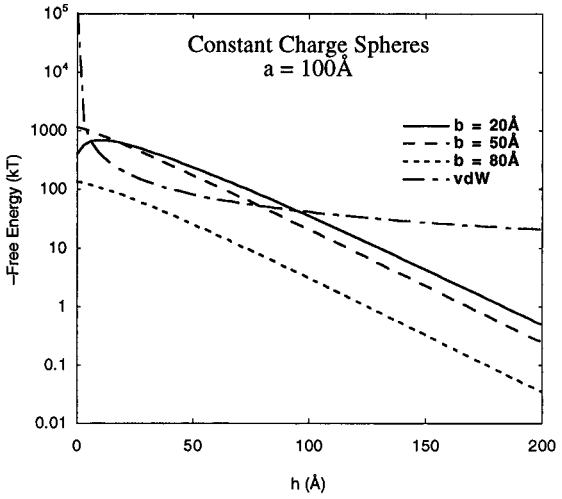

Fig. 2e)

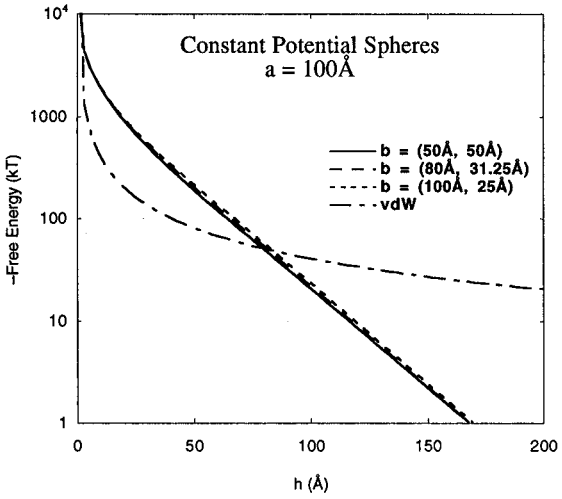

Fig. 2f)

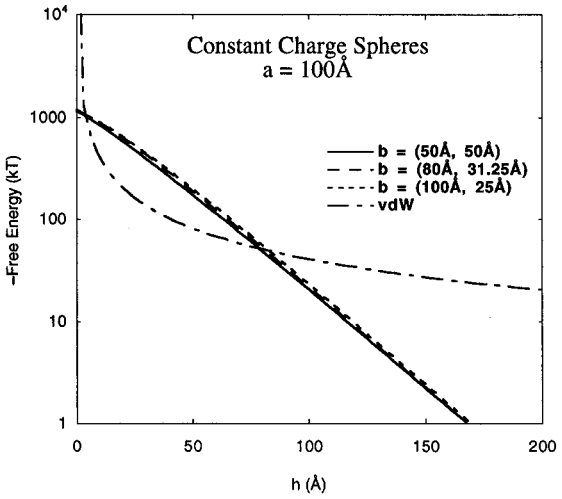

Figure 2. Heterogeneous ($\mathbf{k} \neq \mathbf{0}$) interaction free energy against separation for the two-sphere system, with the spheres out of register with each other ($\mathbf{d} = \mathbf{a}$). (a) and (b) show the effect of modifying the (square) cell size (i.e., the periodicity), keeping the patch size constant ($b_x = b_y = 50$ Å), for constant potential and constant charge boundary conditions, respectively. (c) and (d) show the effect of modifying the (square) patch size, keeping the cell size fixed ($a_x = a_y = 100$ Å). (e) and (f) show the effect of modifying the shape of the patch, keeping its overall area fixed, again with $a_x = a_y = 100$ Å. All systems are in 10^{-2} M electrolyte, with a net potential of 25 mV. The radius of the spheres, R, is taken to be 2 μm. van der Waals energies are included on each graph for comparison, with a Hamaker constant chosen to be 10^{-20} J. Note that the ordinate is the negative of the interaction free energy, so that these figures show attractive interactions.

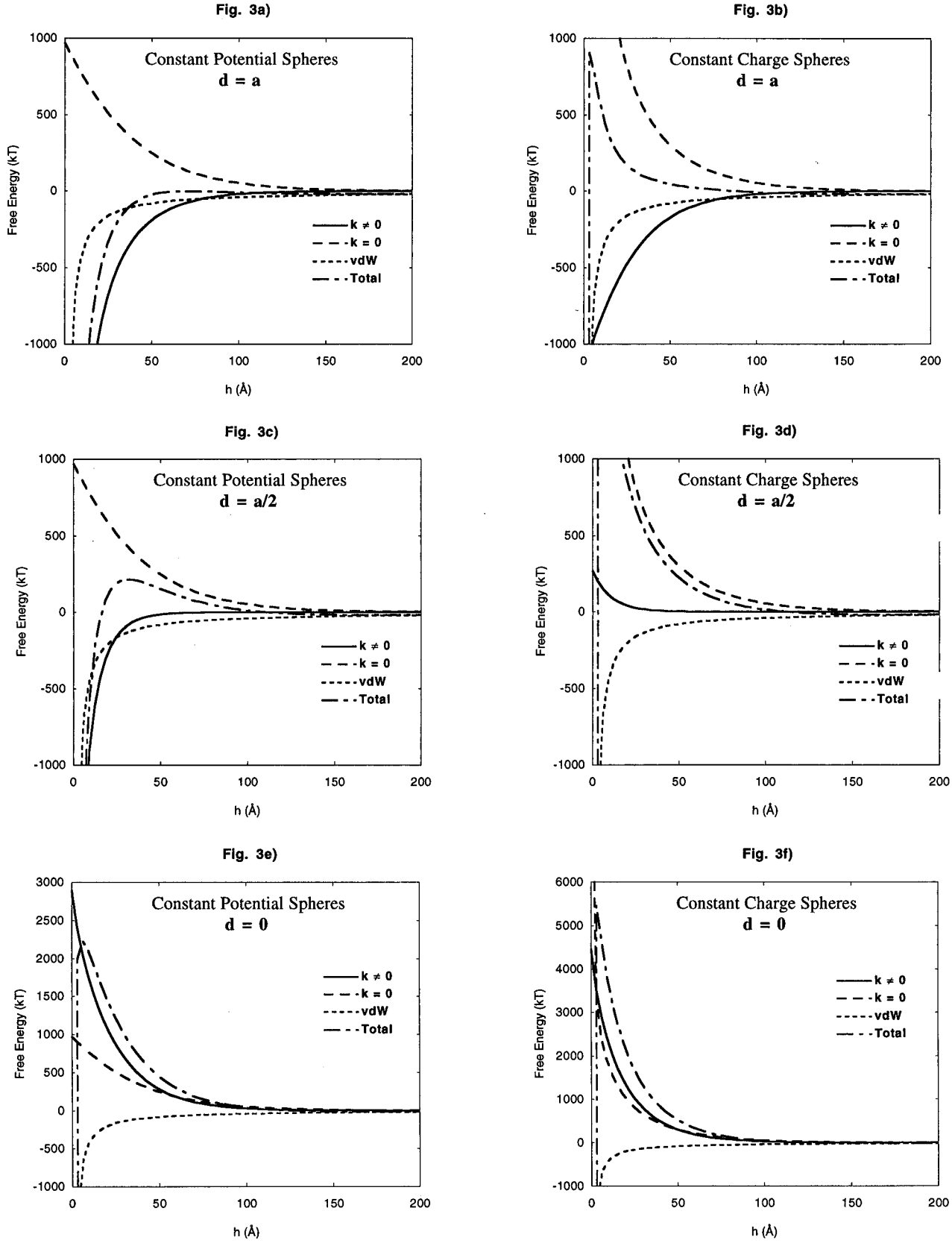

Figure 3. Free energy per unit area versus separation curves, shown broken down into homogeneous electrostatic ($\mathbf{k} = \mathbf{0}$), heterogeneous electrostatic ($\mathbf{k} \neq \mathbf{0}$) and van der Waals (vdW) components. (a) and (b) show the case $\mathbf{d} = \mathbf{a}$ (out of register) for constant potential and constant charge, respectively. (c) and (d) show the corresponding results for $\mathbf{d} = \mathbf{a}/2$, and (e) and (f) show the results for an in register case ($\mathbf{d} = \mathbf{0}$). All results shown are for concentrations of 10^{-2} M, square patches on square cells, with $b_x = b_y =$ 50 Å and $a_x = a_y = 100$ Å. Again, $\psi_{net} = 25$ mV, and $R = 2$ μm.

two surfaces. Constant potential and constant charge results are given for three different lateral displacements: exactly out of register, $\mathbf{d} = \mathbf{a}$; exactly in register, $\mathbf{d} = \mathbf{0}$; intermediate, $\mathbf{d} = \mathbf{a}/2$.

Clearly in the out-of-register systems, the heterogeneous term contributes a substantial attraction. The effective range can also be greater than the van der Waals interactions. As noted above, the effect of the heteroge-

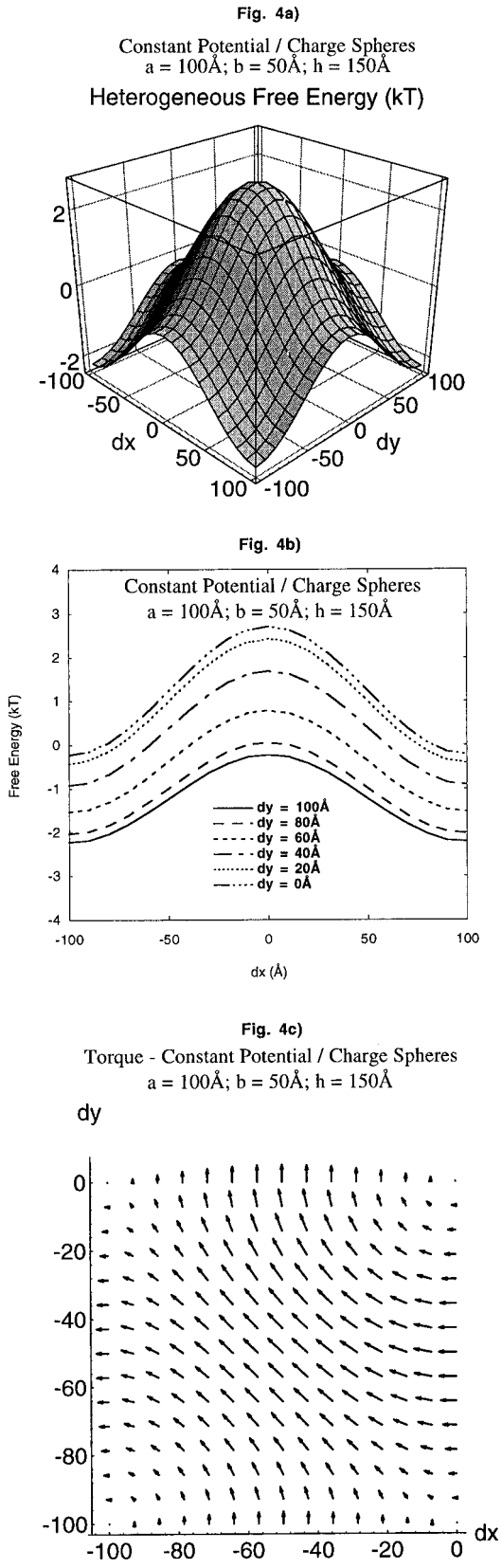

Figure 4. Heterogeneous interaction free energy and torque as a function of plate displacement, **d**, at a spacing of 150 Å. (a) shows 3D representations of the variation in free energy as we shift the spheres over a single lattice spacing relative to each other (for either constant potential or constant charge boundary conditions). (b) shows various cross sections of this curve. (c) shows a torque vector field plot over one quarter of a lattice cell from $\mathbf{d} = (-100\text{ Å}, -100\text{ Å})$ in the bottom left corner to $\mathbf{d} = (0,0)$ in the top right corner. The force is at right angles to the torque and is directed toward the energy minima. Scaling for Figure 4c: The center top arrow (at $\mathbf{d} = (-50\text{ Å}, 0)$) is of magnitude $919kT$.

neity is more pronounced in the constant potential case than in the constant charge examples. The intermediate ($\mathbf{d} = \mathbf{a}/2$) case, as expected, differs little from the classical DLVO result, although in the constant potential case, a noticable attraction is evident. In the in-register configuration ($\mathbf{d} = \mathbf{0}$) there is an additional repulsive contribution from the heterogeneous term which is of similar magnitude to the attraction in the out-of-register systems; this results in a far greater repulsion than a purely homogeneous surface would exhibit.

These results are all as one would expect. When patches on one surface face the patches on the other, the repulsion ought to be greater than if those patches were "spread out". If the patches are misaligned, so that the patches on one surface see predominantly background material on the other, an additional attraction would be expected. The interaction free energy of a two sphere system with square lattice patches is a minimum when $\mathbf{d} = \mathbf{a}$ and a maximum when $\mathbf{d} = \mathbf{0}$.

The variation of the interaction free energy as a function of displacement **d** is shown in Figures 4 and 5. Again, these curves represent only the heterogeneous ($\mathbf{k} \neq \mathbf{0}$) components of the energy; the DLVO terms will be a constant value for any graph, since these are evaluated at fixed values of the separation h. In Figure 4 we show results for $h = 150$ Å, where the spheres are separated by a distance roughly corresponding to the location of the secondary DLVO minimum. At this large separation, the results for constant potential and constant charge boundary conditions are indistinguishable. Given that the results approach each other as the separation increases, at this separation they are identical to within our resolution. In Figure 5 we give results at a small plate separation of 20 Å. Figures 4a, 5a, and 5b are three-dimensional plots showing the heterogeneous free energy per unit area as a function of d_x and d_y, the displacement components (for constant potential and constant charge, respectively), while Figures 4b, 5c, and 5d show two-dimensional cross sections of these plots.

In Figure 4 we see the expected free energy surface which exhibits a maximum at $\mathbf{d} = \mathbf{0}$ and minima at the four corners, where $|\mathbf{d}| = |\mathbf{a}|$. The displacement grid shown corresponds to a twisting of the spheres by one lattice spacing relative to each other. The section curves for constant potential and constant charge are practically indistinguishable. At this separation, $h = 150$ Å, the free energy when averaged out over all displacements is very close to zero. Figure 4c shows actual torque lines as a function of displacement, running over one quarter of a single lattice cell; the remainder of the cell can be obtained by symmetry. The torques shown correspond, as expected, in a force toward the free energy minimum; the out of register alignment with $|\mathbf{d}| = |\mathbf{a}|$. The torque reaches a maximum when the lattices are half-aligned (i.e., $|\mathbf{d}| = |\mathbf{a}/2|$). This is effectively the "restraining torque" on the pair, as it is the torque required to enable the spheres to rotate freely. The magnitude of this torque can easily be of the order of thousands of kT, even at separations comparable to the secondary DLVO minimum.

With the spheres held at a smaller separation, $h = 20$ Å (Figure 5), the constant potential case averages out to a net attraction, while the constant charge case averages to a net repulsion. Although the extreme cases (exactly in or out of register) still result in repulsion and attraction respectively for either boundary condition, the intermediate alignments can give differing behavior for the two boundary conditions. The corresponding torques are shown in parts e and f of Figure 5. Naturally, at this lower separation, these torques will have far higher values, reaching hundreds of thousands of kT. Note also that the

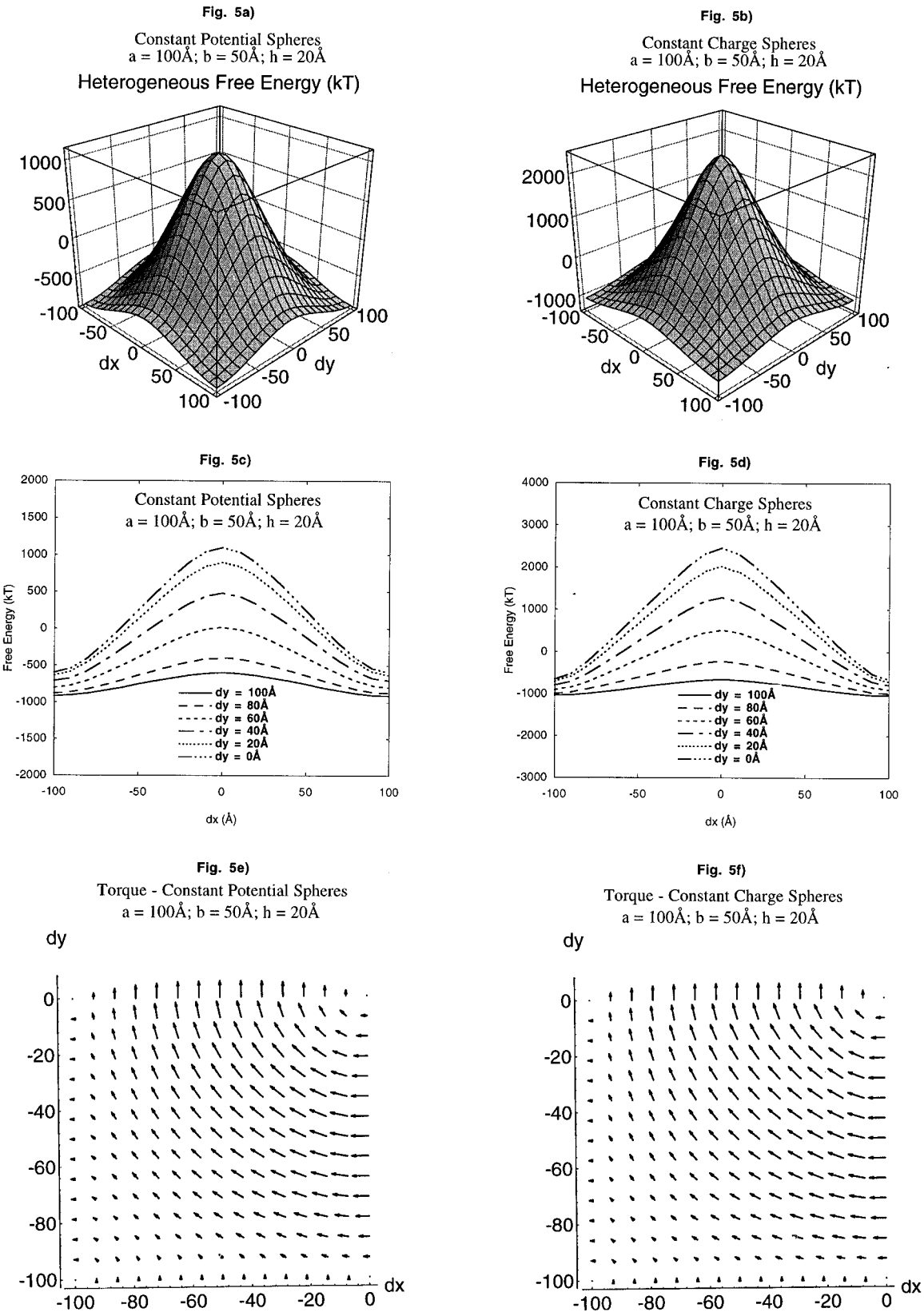

Figure 5. As for Figure 4, but at 20 Å separation. Here the constant potential and constant charge boundary conditions give distinctly different results. (a) and (b) show 3D plots of the free energy against displacement; (c) and (d) show cross sections of these curves; (e) and (f) are torque vector field plots. Scaling for Figure 5e: The center top arrow has magnitude $4.62 \times 10^5 kT$. Scaling for Figure 5f: The center top arrow has magnitude $7.77 \times 10^5 kT$.

sharper peak for the constant charge free energy results in higher values of the torque than in the corresponding constant potential case. Also note that in both cases, it takes far more work to twist the system through the maximum than to misalign the system in just one dimension, twisting along one of the axes.

The results lead to some interesting conclusions. While the model appears artificial in its square, periodic geometry, it does appear that the square patch configuration gives a lower bound for rectangular periodic patches. And if the spheres arranged themselves so as to minimize the free energy, attractions of longer range than van der

Waals attractions are likely. The range of these heterogeneous attractions is determined by the cell size; in other words the periodic length scale of the surfaces controls the decay length of the extra heterogeneous contribution. Additionally, restraining torques of extremely large magnitudes can be found, even at separations which are of at least the order of the cell size.

5. Conclusion

Recent experimental evidence suggest the existence of unexplained forces and restraining torques upon colloidal surfaces. Using a periodic patchy model of charge heterogeneity, we have been able to obtain substantial additional attractive free energies between pairs of identical spheres, of a similar nature to that obtained between pairs of heterogeneous plates, if the lattices are arranged to be out of alignment. These attractions have a modified decay length which varies with the period of heterogeneity and can therefore have a far greater range of significant effect than van der Waals attractions. Furthermore, very large restraining torques are found, even at relatively low free energies and significant separations, for example, at the secondary DLVO minimum. This is a phenomenon completely absent from DLVO theory and suggests that heterogeneous systems may lie at the heart of restraining torques found experimentally.

Acknowledgment. This work was supported by an Australian Postgraduate Award by the Australian Research Council Special Research Centre, the Advanced Mineral Processing Centre, and by an Australian Research Council Large Grant. We thank Professor John L. Anderson for suggesting a number of facets of this problem to explore.

LA960389X